Journal of Applied Polymer Science

Preparation and assessment of a self-healing material based on microcapsules filled with ethyl phenylacetate

Wanpeng Ma, Wei Zhang, Yang Zhao, Helong Yu
Science and Technology on Remanufacturing Laboratory, Academy of Armored Forces Engineering, Beijing 100072, China
Correspondence to: W. Zhang (E-mail: zhangwei18@hotmail.com)

ABSTRACT: A self-healing material was developed on the basis of a biological system. The self-healing epoxy resin, which incorporated microcapsules filled with ethyl phenylacetate (EPA), was investigated. The microcapsules were prepared by an *in situ* polymerization method. The microcapsule-formation process was monitored by optical microscopy, and the surface morphology was observed by scanning electron microscopy (SEM). The self-healing performance of the epoxy resin was assessed by manual and *in situ* healing experiments. We investigated the effects of the healing time, amount of EPA, and degree of curing of matrix on the healing performance by manually injecting EPA into the crack plane. The maximum healing efficiency was obtained within 24 h. The swelling curve was overlaid onto the healed load plot; this indicated that crack healing was achieved as a result of solvent diffusion. The healing load reached the maximum value when the amount of EPA was 0.5 μL and was capable of filling the crack volume. Moreover, the healing performance was related to the degree of swelling. The *in situ* healing efficiency was dependent on the microcapsule concentration. The fracture toughness could be fully restored when the microcapsule concentration was 10%. Finally, the crack interface was analyzed with SEM. The results show that the fracture line was difficult to detect, and this suggested complete crack healing by EPA.
 J. Appl. Polym. Sci. **2016**, *133*, 43430.

KEYWORDS: biomaterials; biomimetic; stimuli-sensitive polymers; swelling; thermosets

Received 25 April 2015; accepted 9 January 2016
DOI: 10.1002/app.43430

INTRODUCTION

Polymers have been widely used in the aerospace, automotive, and ship industries because of their high specific strength, high stiffness, high modulus, and corrosion resistance.[1–3] However, polymers are susceptible to exterior and interior damage, particularly microcracks deep in the structure, during manufacturing and use. If this damage is not repaired, the presence of microcracks causes a decline in the overall performance of the structure, and the propagation of microcracks can lead to catastrophic failure. However, conventional nondestructive testing technologies, such as ultrasound, IR thermography, and X-ray tomography, have difficulty detecting microcracks. Therefore, the detection and repair of microcracks are very important.

Inspired by the self-healing system of organisms, scientists have proposed the concept of self-healing materials that can detect damage and heal it automatically.[4–8] Research on microcapsule self-healing materials has become a hot spot in recent years because of these materials' matured manufacturing, small influence on matrix properties, and great application potential.[5,9–11] The repair process is triggered by the rupture of microcapsules when a crack propagates through the matrix; this is followed by release of the healing agent into the crack plane. The healing agent then mixes with the catalyst and bonds the crack through polymerization. Several materials can be used as healing agents on the basis of their different healing chemistries; these include dicyclopentadiene,[12–16] vinyl terminated poly(dimethyl siloxane) resin,[17,18] epoxy resins,[19–24] and solvents.[25–29] Compared with other healing systems, the solvent-promoted self-healing system is a simple, one-component, less expensive, and highly efficient system because of the absence of catalysts. Although crack healing in thermoplastics has been investigated primarily because of the diffusion of chains across the interface,[30–32] the healing mechanism of a thermoset based on a solvent remains unclear. The results have shown that solvent-based systems rely on matrix swelling; this allows intimate contact between the crack and the remainder of the material and promotes the reaction of residual functionalities induced by the solvent.[28] The healing performance in terms of the healing time, amount, and degree of curing is relative to the swelling process. However, limited investigation on the healing performance on the basis of the swelling mechanism has been performed. Systematic information on the influence of such factors on the healing efficiency

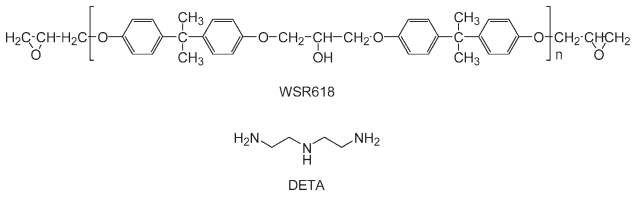

Figure 1. Chemical structure of the epoxy resin and hardening agent used in this work.

can facilitate the optimization of the formulation and design for the further practical application of solvent-promoted systems; thereby, deep investigation is needed.

In this study, the solvent ethyl phenylacetate (EPA) was selected as a healing agent, and microcapsules were prepared by an *in situ* polymerization method. The microcapsule-formation process and surface morphology were examined. The self-healing materials were prepared by the incorporation of a microcapsule of EPA into the matrix (epoxy resin). The effects of the healing time, amount, and degree of curing of the matrix on the healing efficiency were investigated through manual healing experiments. The relationship between the swelling and healing efficiency was demonstrated. Furthermore, the *in situ* self-healing efficiency was investigated.

EXPERIMENTAL

Materials

The microcapsule wall-forming materials urea and ammonium chloride were purchased from Tianjin Fengchuan Chemical Reagent Technologies Co., Ltd. (China). Formalin (37% formaldehyde in water) solution and resorcinol were purchased from Xilong Chemical Co., Ltd. (China). The ethylene–maleic anhydride (EMA) copolymer surfactant was purchased from Sigma–Aldrich. Distilled water was used to prepare the aqueous solutions. A 10% NaOH solution was used to adjust the pH. The epoxy resin, WSR618 (its properties are the same as those of Epon 828), was purchased from Nantong Xingchen Synthetic Material Co., Ltd. (China). The hardening agent, diethylenetriamine (DETA), was obtained from Xilong Chemical Co., Ltd. (China). EPA (99%), the healing agent, was purchased from Aladdin. All chemicals were used without further purification. Figure 1 shows the chemical structures of WSR618 and DETA.

Preparation of the Microcapsules

The microcapsules were synthesized with an *in situ* polymerization procedure with slight modifications.[33] Exactly 1.25 g of EMA was dissolved in 50 mL of deionized water in a warm bath to obtain a 2.5% aqueous surfactant solution. The wall-forming materials of the microcapsule (5 g of urea, 0.5 g of ammonium chloride, and 0.5 g of resorcinol) were placed in a 500-mL beaker at room temperature, and then, 200 mL of deionized water and the previous surfactant solution were added. The pH was adjusted from approximately 2.6 to 3.5 by the addition of an NaOH solution, and then, 90 mL of EPA was added to the solution to form an oil–water emulsion, which was agitated with an emulsification isotropic machine. Subsequently, the beaker was suspended in a temperature-controlled water bath and agitated with a digital mixer (IKA RW20, Eurostar). Finally, 12.67 g of formaldehyde solution was added to the mixing solution, and the obtained solution was heated to 55°C at a rate of 1°C/min. After 4 h of continuous heating, the microcapsules were rinsed with deionized water, immediately separated with a filter, and then air-dried for several days.

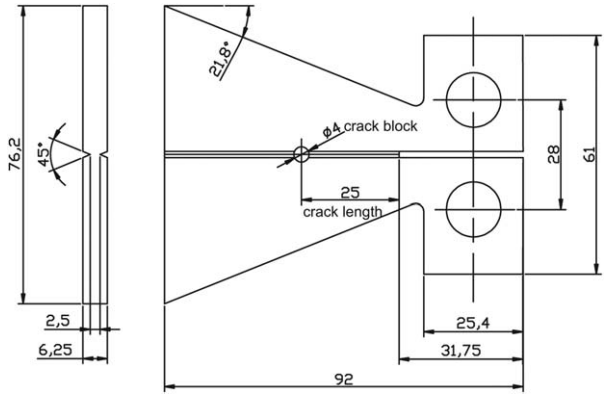

Figure 2. Modified TDCB geometry.

During the microencapsulation process, drops of reaction solution were dripped onto glass slides at specified intervals, and the wall-forming process was observed by optical microscopy (DP12, OLYMPUS). The surface morphology was examined by scanning electron microscopy (SEM; QUANTA200, FEI) at low-vacuum mode. The dried microcapsules were mounted on conductive carbon tape and then sputtered with a thin layer of gold-palladium to prevent charging under the electron beam.

Taper Double-Cantilever Beam (TDCB) Specimen Preparation

With the protocol established by White *et al.*,[9] the healing performance of EPA was assessed by fracture toughness analysis of the TDCB epoxy resin specimens. After complete fracture, the fracture planes had to be realigned and allowed to be in close contact to realize the healing process with the assistance of a clamp. To eliminate the errors of pressure and alignment caused by the clamp, a modified TDCB specimen was designed to prevent the fracturing of the specimen into two parts. A hole was introduced as a crack block on the propagation pathway of the crack, as shown in Figure 2. The hole was located 25 mm away from the starter notch; thus, a 25-mm crack had to be healed.

Two types of healing experiments were conducted: manual healing and *in situ* healing experiments. For the manual healing experiment, the specimens were prepared at with a 100:12 parts per hundred WSR618/DETA mixture; this ratio corresponded to the stoichiometric ratio. The epoxy mixtures were degassed, poured into silicone molds, and underwent the specified curing conditions (Table I). Except when the influence of the degree of curing on the healing performance was investigated, the curing

Table I. Curing Conditions

Designation	Set
Curing condition 1	RT × 24 h + 35 °C × 24 h[a]
Curing condition 2	RT × 24 h + 40 °C × 24 h
Curing condition 3	RT × 24 h + 40 °C × 24 h + 70 °C × 3 h

[a]RT represents room temperature (18–22 °C).

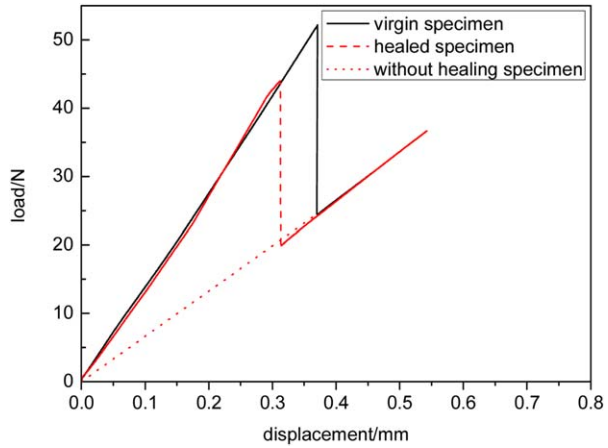

Figure 3. Typical load–displacement curve for the virgin, healing, and nonhealing specimens. [Color figure can be viewed in the online issue, which is available at wileyonlinelibrary.com.]

conditions were 24 h at room temperature followed by 24 h at 35°C (curing condition 1). For the *in situ* healing experiment, the microcapsules filled with EPA were stirred into the epoxy resin mixture at various concentrations by weight, and the remaining preparation process was the same as that of the manual healing specimens.

Self-Healing Experiment

The specimens were precracked with a razor blade and then pin-loaded onto a Bose 3100 frame under displacement control at a rate of 0.3 mm/min. When the crack propagated the hole, as indicated by a sudden load decrease in the load–displacement curve, the specimens were unloaded, and the crack planes were allowed to be in close contact for healing. The self-healing performance of the epoxy resin was assessed by manual healing and *in situ* healing experiments.

Through the manual healing experiment, the factors influencing the healing efficiency (healing time, solvent amount, and degree of curing) were investigated; we ignored the delivery efficiency of the healing agent caused by the microcapsule. After fracture, a specific amount (from 0.1 to 5 μL) of solvent was injected into the crack plane with a microsyringe. The specimens were allowed to heal for a given time at room temperature. Afterward, the healed TDCB specimens were loaded in a similar manner, and the load–displacement curve was recorded. In the case of the *in situ* healing experiment, the specimen was observed without manual interruption after the fracture experiment and then loaded to test the *in situ* healing efficiency. Each batch included five specimens so that we could obtain an average value.

Assessment of the Healing Performance

A typical load–displacement curve is shown in Figure 3. The healing performance was assessed by the peak load, as indicated by the jump point. The healing efficiency is usually estimated through a comparison of the virgin and healed fracture toughness, as proposed by White *et al.*[9] The TDCB geometry was calculated as simply the ratio of the peak loads for the healing and virgin specimens:

$$\eta = \frac{K_{IC\text{healed}}}{K_{IC\text{virgin}}} = \frac{P_{IC\text{healed}}}{P_{IC\text{virgin}}} \quad (1)$$

Where $K_{IC\text{healed}}$ and $P_{IC\text{healed}}$ is the fracture toughness and peak load of the healed specimen respectively, $K_{IC\text{virgin}}$ and $P_{IC\text{virgin}}$ is the fracture toughness and peak load of the virgin specimen respectively. The slope of the load–displacement curve was also used to quantify the healing performance.[34] The slope of the curve decreased suddenly when the crack propagated to the hole. Because of the healing process, the slope recovered to the value before the crack propagated to the hole. When the healing process did not happen, the slope was identical to the slope of the curve after the crack propagated to the hole.

Swelling Experiment

The swelling experiment was conducted to quantify the degree of swelling of the epoxy resin immersed in the solvent. The preparation of the specimen was similar to that of TDCB. The dimensions of the specimen were $16 \times 10 \times 5\ \text{mm}^3$. After they were removed from the silicone molds, the specimens were weighed by a Mettler 350 balance and then placed into 100-mL vials containing the solvent. After they were immersed for 24 h, we took the specimens out of the solvent, wiped off the excess solvent, and measured the weight after swelling. The *relative mass gain* was defined as the ratio of the gained mass and the initial mass. Each group of data included seven specimens to yield an average value.

Thermal Analysis

To quantify the effects of the curing conditions on the glass-transition temperature (T_g) and degree of curing, differential scanning calorimetry (DSC; TA Q100) was performed on the fresh and cured epoxy samples. Approximately 10-mg samples were cured in aluminum pans under different curing conditions. All of the samples were tested with a temperature ramp from 25 to 250°C at 10°C/min. We also measured the total polymerization heat by placing a freshly mixed resin–hardener droplet on the aluminum pan and immediately starting the same temperature ramp used previously. The degree of curing (α) was determined by the following equation:

$$\alpha = 1 - \frac{\Delta h_{\text{res}}}{\Delta h_{\text{total}}} \quad (2)$$

where Δh_{res} is the residual heat evolved during postcuring and Δh_{total} is the total heat of polymerization taken from dynamic scans.

Crack Interface after Healing

To obtain the crack interface, the specimen was cut perpendicular to the crack direction after the healing process. The interface was examined with an SEM instrument (QUANTA200, FEI) after sputter-coating treatment with a gold source.

RESULTS AND DISCUSSION

Microcapsule-Formation Process

To reveal the microcapsule-formation mechanism, the formation process was monitored for different reaction times, as shown in Figure 4. Before 45 min, droplets of oil were dispersed stably in the solution. At 60 min, the aqueous solution became opaque and cloudy because of the increase in the molecular weight and decrease in the solubility of the UF (urea-formaldehyde)

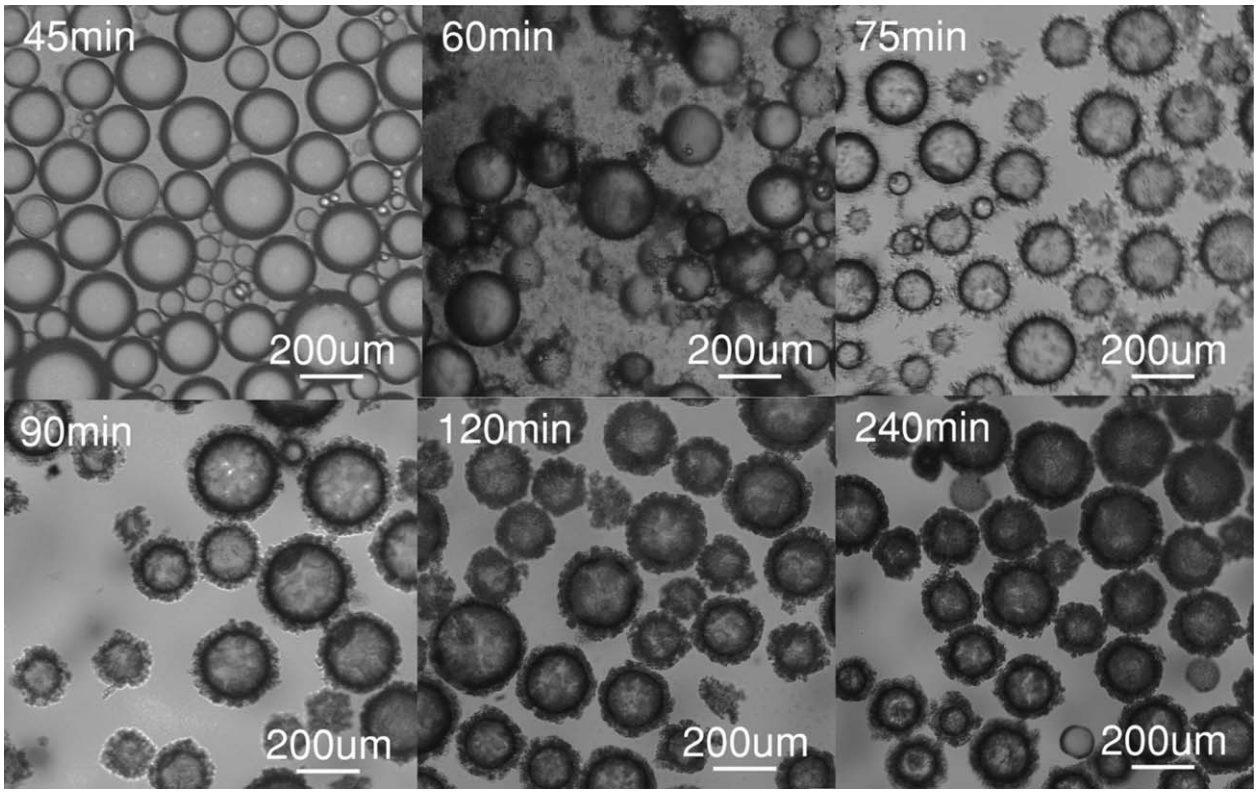

Figure 4. Optical micrographs of the microcapsule-formation process with EMA as an emulsifier at different reaction times.

prepolymer.[35] To clarify the image, the solution was diluted by the addition of deionized water. After 75 min, the image showed a sharply different surface morphology of microcapsules, and the smooth surface of the droplets began to show some setae; this indicated the deposition of the UF prepolymer on the surface of the droplet. The setae on the surface of the droplet became denser at 90 min because more UF prepolymer was absorbed on the surface. After 2 h, no obvious changes were observed, and the microcapsule wall solidified and crosslinked further.

The microcapsule-formation process could be subdivided into three stages on the basis of the microcapsule morphology.

Emulsification Stage. In the first stage, emulsification, EPA was dispersed stably in the solution as a result of the emulsifier EMA. Because the anhydride moiety and the ethylene unit of EMA were rather similar in size, they were absorbed on the oil–water interface. In addition, the surface of the oil droplet became negatively charged because of the carboxyl group, which stabilized the emulsion by electrostatic repulsion and steric repulsion.[36]

Wall-Formation Stage. Polymerization between urea and formaldehyde was initiated in the water phase with the aid of acid to form a low-molecular-weight prepolymer. The solubility of the prepolymer decreased and the aqueous solution turned milky white with increasing molecular size. Because the EMA molecules had several carboxyl groups, they catalyzed the polymerization and worked as a reaction site for the polymerization of urea and formaldehyde.[37] Thus, the prepolymer was deposited at the oil–water interface, and the smooth surface was covered with spines; this indicated the deposition of the UF polymer.

Wall-Solidification Stage. In third stage, the wall thickness no longer increased, and the polymerization reaction between urea and formaldehyde ran further at the oil–water interface to form a highly crosslinked wall. In addition, the microcapsules were extremely fragile at the start of the wall-solidification stage. When the microcapsules were separated from the reaction vessel after very short periods, they collapsed, even during the drying process.

Microcapsule Surface Morphology

The microcapsules had a rough outer surface and a smooth, nonporous inner wall, as shown in Figure 5; this was indicated by the microcapsule-formation process. The smooth, nonporous inner surface was believed to be the result of the deposition of the low-molecular-weight prepolymer at the oil–water interface.[36] This would provide it with a long shelf life. A rough surface morphology was formed when the UF nanoparticles were deposited at the interface. This condition was helpful for improving the bonding strength between the microcapsule and the matrix and increased the probability of the reaction rupturing capsule rather than just pulling out the entire capsule. This increased healing agent delivery and healing efficiency.

Factors Affecting the Manual Healing Performance

When the crosslinking polymer came into contact with EPA, the EPA molecules swelled the polymer and allowed intimate contact between the crack faces. Then, the solvent enhanced the reaction of the epoxy functionalities with the unreacted

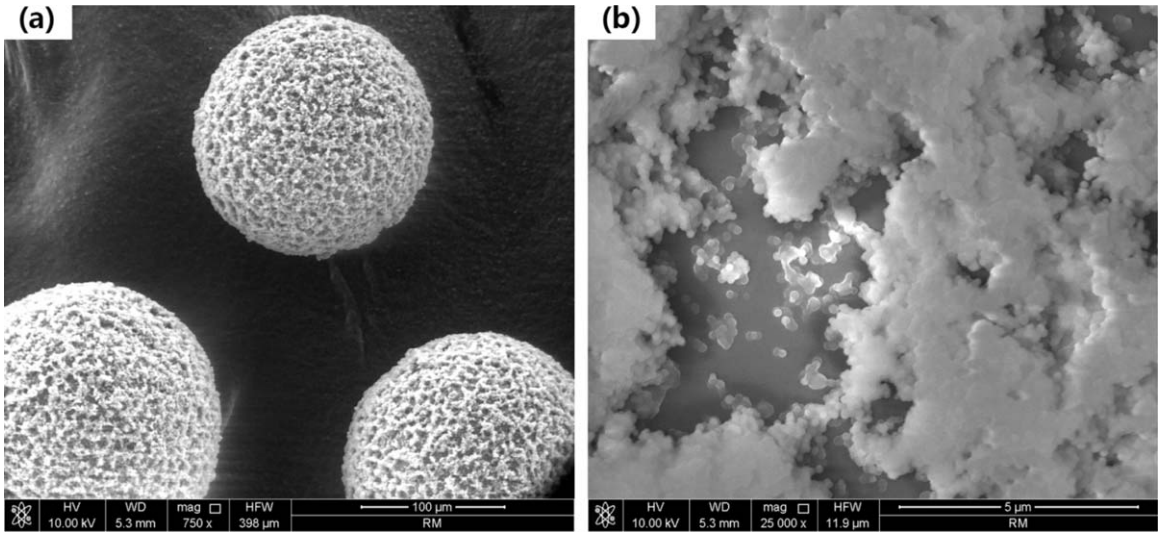

Figure 5. SEM images of the microcapsules containing EPA: surface morphologies of the (a) microcapsules and (b) partial enlargement.

hardener functionalities in the swollen matrix region.[28] The healing process revealed that the healing performance was dependent on the healing time, the amount of healing agent, and the degree of curing of the matrix. To eliminate the effect of microcapsule delivery on the healing efficiency, these influencing factors were investigated through manual healing experiments.

Manual Healing Performance: Effect of the Healing Time

The healing process revealed that the healing rate should have been correlated to the swelling rate. Therefore, the healing rate was compared with the swelling rate, which was measured by immersion in EPA. The healed load of EPA increased over time, as shown in Figure 6. It was then overlaid on the swelling rate plot. The amount of healing agent was 0.5 μL, which was sufficient for healing. The healing efficiency had a certain relationship with the solvent diffusion in the matrix. At the start of 6 h, the growth of the healing load was relatively quicker because of the faster rate of solvent diffusion. The concentration of the healing agent was saturated in the crack region after 24 h, so the solvent no longer spread among the matrix, and the healed load did not show any increase. Therefore, 24 h was chosen to ensure sufficient time for healing; the peak load healed for 24 h was 49 N. Because the peak load of the virgin specimen was 54 N, the manual healing efficiency was 90.4%.

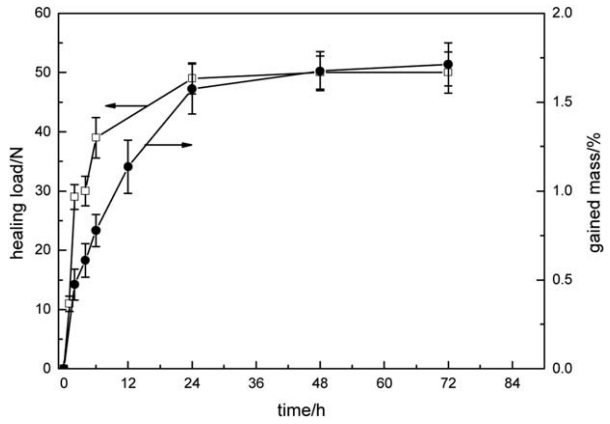

Figure 6. Time dependence of the healed load in comparison with the swelling rate plot (amount of healing agent = 0.5 μL).

Further examination of the load–displacement curve (Figure 7) showed more details about the healing process. Stick–slip behavior was observed during propagation in the healing specimen for 1 h; this indicated that the crack stopped propagating because the solvent diffused into the matrix and plasticized the crack region.[38] With time, the slope of the curve increased and showed brittle failure because the bond strength became stronger; this was induced by the solvent.

Manual Healing Performance: Effect of the Amount of the Healing Agent

Figure 8 shows that the self-healing performance depended on the amount of healing agent injected into the crack plane. When the amount of healing agent was less than 0.5 μL, the healed load increased rapidly. The healing load increased slightly

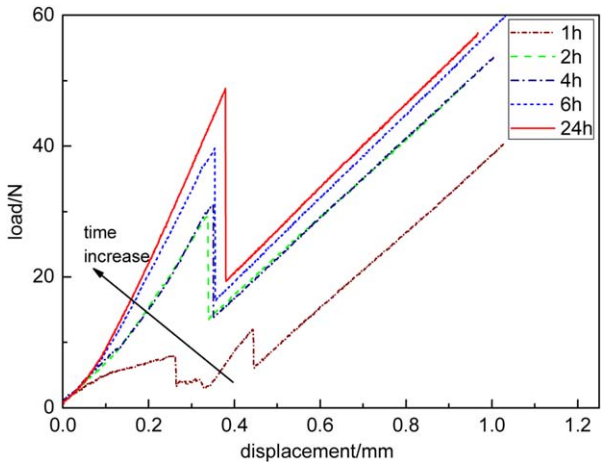

Figure 7. Load–displacement curves for different healing times. [Color figure can be viewed in the online issue, which is available at wileyonlinelibrary.com.]

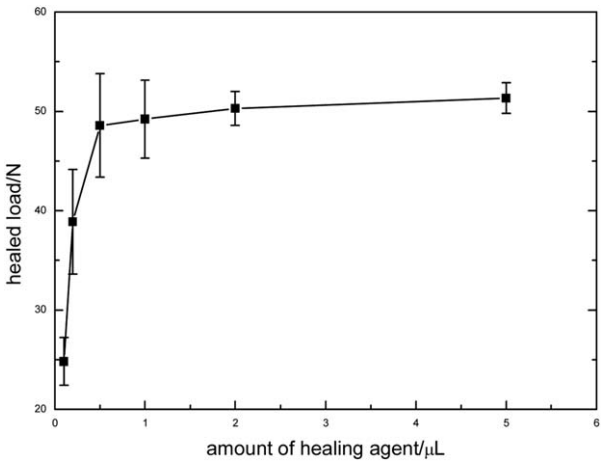

Figure 8. Influence of the amount of healing agent on the healing load (healing time = 24 h)

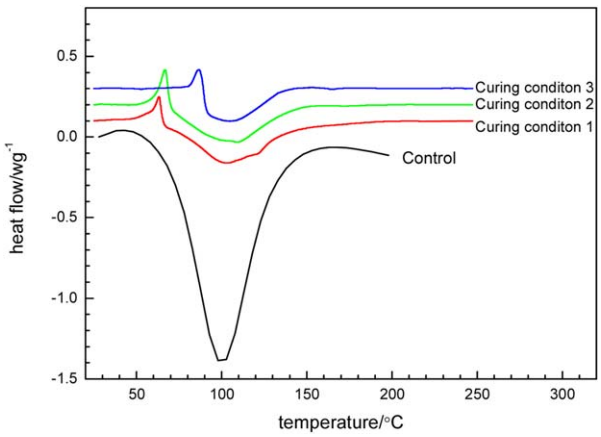

Figure 10. DSC result for an epoxy resin under different curing conditions. [Color figure can be viewed in the online issue, which is available at wileyonlinelibrary.com.]

when the amount of healing agent was greater than 0.5 μL. The crack separation in the fractured TDCB specimens was examined by SEM to determine the amount of required healing agent, as shown in Figure 9. The average crack separation was 5.84 μm. The crack length and width of the TDCB specimens was 25 and 2.5 mm, respectively. Thus, the crack volume was 0.365 μL. When the volume released could fill the crack volume, the healing efficiency reached the maximum value. However, excessive healing agent no longer increased the healing efficiency. Thus, the amount of healing agent injected into the crack was 0.5 μL, unless otherwise stated.

Manual Healing Performance: Effect of the Degree of Curing

Three different curing conditions (Table I) were applied to investigate the effect of the degree of curing on the healing efficiency. T_g and the degree of curing of the sample were determined by DSC. Figure 10 shows the DSC results of the cured epoxy samples. With curing condition 1 taken as an example, an enthalpic relaxation peak, which could be estimated from the actual T_g, at 63°C was observed and then was immediately followed by an exothermic peak because of the residual heat of the reaction. The residual heat of the reaction was 71 J/g, whereas the total heat of polymerization was 264 J/g; therefore, the degree of curing was 73% according to eq. (2). With increasing curing time and temperature, T_g and the degree of curing increased, as listed in Table II. The relationship between T_g and the degree of curing was consistent with the result of Francos.[39]

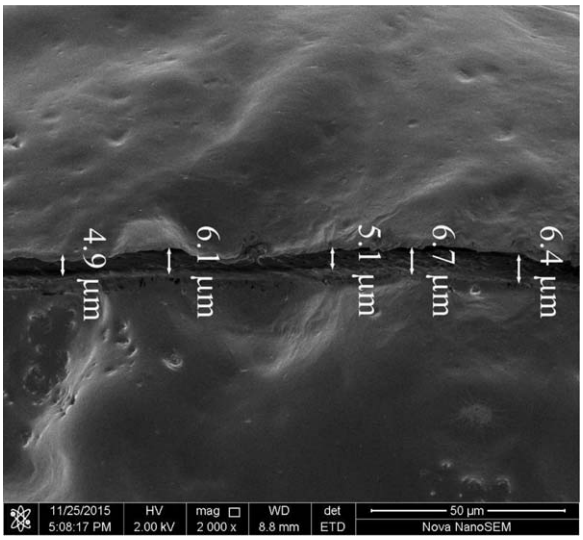

Figure 9. SEM images of a crack under autonomic repair.

The relationship between the healed load and degree of curing is demonstrated in Figure 11(a). Ethanol and acetone were selected as healing agents because of their different swelling abilities. When the degree of curing was 73% (curing condition 1), the healing load of EPA was 53 N. However, the healing process did not take place entirely when the degree of curing was 82% (curing condition 3). The healing performance of acetone and ethanol followed similar rules. The healing performance of the three healing agents appeared to be inversely related to the degree of curing.

Because the healing efficiency in terms of the healing time and amount was relative to the swelling process, we expected that the healing performance in terms of the degree of curing would also be relative to the swelling. The degree of swelling was measured to validate this assumption. The swelling ability of the solvents were all inversely related to the degree of curing (or T_g), as shown in Figure 11(b). When the degree of curing was high and the molecular mobility (as indicated by T_g) was low, the extent of solvent-induced swelling became small. The previous results show that the healing performance depended on the

Table II. T_g and Degree of Curing under Different Curing Conditions

Curing condition	T_g (°C)	Δh_{res} (J/g)	Degree of curing (%)
Control	—	264	—
Curing condition 1	63.1	71	73
Curing condition 2	66.8	60	77
Curing condition 3	86.8	47	82

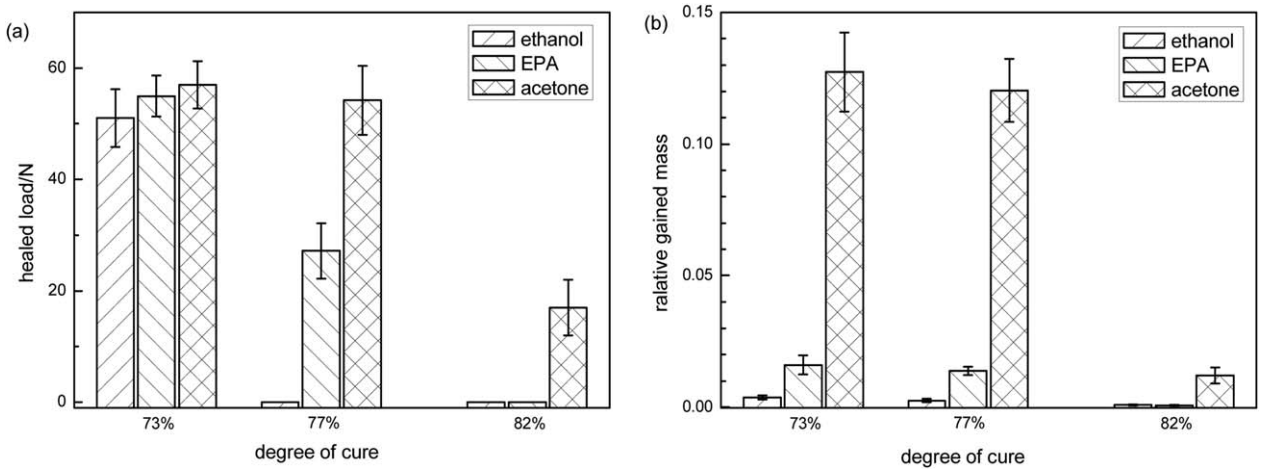

Figure 11. Effect of the degree of curing on the healed load and relative gained mass: (a) healed load for an epoxy resin under different curing conditions with ethanol, EPA, and acetone as healing agents and (b) relative gained mass of an epoxy resin under different curing conditions after immersion in ethanol, EPA, and acetone.

degree of swelling. The decrease in the healing efficiency when the degree of curing increased was attributed to the decrease in the degree of swelling. A low swelling ability led to an incompletely swollen matrix and partly increased the molecular mobility; thereby, mechanical restoration was partly obtained.

Therefore, the solvent-promoted healing systems had a fatal flaw, which partially or fully diminished the healing ability responsible for the swelling mechanism compared with the dicyclopentadiene/Grubbs or the epoxy/harder healing system, which is not sensitive to the degree of curing of the matrix. When the sample was highly crosslinked, the solvents partially or fully diminished the healing ability responsible for the swelling mechanism. A comparison of Figures 11(a) and 11(b) shows that the solvent with a high swelling capacity had a better healing performance for the same degree of curing. To obtain a high healing efficiency, solvents with a high swelling capacity (e.g., acetone) need to be selected as healing agents. The autonomic self-healing material requires that a solvent can be encapsulated and that the capsules are embedded in the epoxy matrix. Unfortunately, acetone is soluble in water; hence, it is difficult to use in microcapsule preparation. In future research, we will focus on the selection of solvents with good swelling abilities than can be simultaneously encapsulated.

Influence of the Microcapsule Concentration on the Healing Load and Healing Efficiency

To test the *in situ* healing efficiency, a microcapsule/epoxy resin composite was prepared by the addition of microcapsules into the epoxy resin matrix. As illustrated in Figure 12, the addition of microcapsules showed no obvious influence on the fracture toughness of the composite materials and thus did not reduce the fracture toughness of the composite. Nevertheless, the microcapsule concentration had obvious effects on the healing load and healing efficiency. With increasing microcapsule concentration up to 10%, the healing efficiency increased. However, the healing efficiency decreased when the concentration was greater than 10%. When the concentration was 10%, the healing efficiency could reach about 100%. This result shows that the fracture toughness of the materials could be fully restored to its original form under certain conditions. When the concentration was increased to 15%, the healing efficiency decreased to 81.0%. This trend was in agreement with the manual healing experiment results and suggested that excessive microcapsules did not improve the healing efficiency further.

Crack Interface after Healing

To examine the structure of the interfaces bonded by solvent, a longitudinal cross section of the healing specimen was cut. When the healing efficiency was low (e.g., the concentration of microcapsules was 2%), the interfaces were fragile and fractured into two parts in the process of cutting. Therefore, the crack interface of the self-healing material filled with 10% microcapsules (healing efficiency = 100%) is displayed in Figure 13. Before healing, a visible crack was found in the specimen. After healing, the fracture line in the healed region was hard to detect; this suggested complete crack healing by the solvent. After the microcapsules were ruptured when a crack was propagated through the matrix, solvents were released into the surface

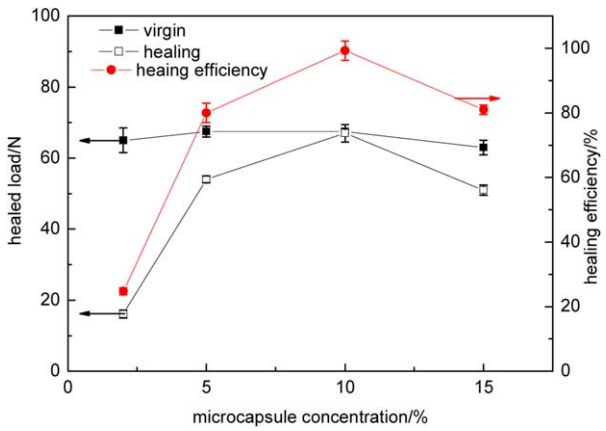

Figure 12. Influence of the microcapsule concentration on the healing load and healing efficiency. [Color figure can be viewed in the online issue, which is available at wileyonlinelibrary.com.]

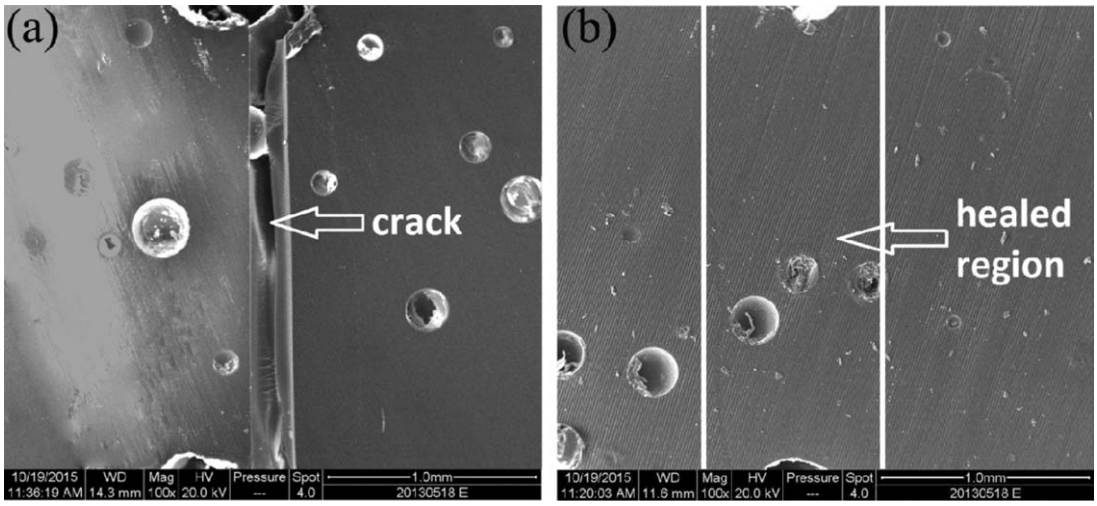

Figure 13. Crack interface of a self-healing material filled with 10% microcapsules (a) before and (b) after healing.

areas; these swelled the crack region and allowed closure of the crack by the swelling effect. The crack was healed by an increase in the molecular mobility in the swollen regions and promoted the reaction of residual functionalities. Surprisingly, this uniform structure was different from the healing interface of thermoplastics, in which exist a soft, residual final adhesive layer induced by solvent diffusion,[40] because the swelling degree of the thermoset (epoxy resin) was small compared with thermoplastics.

CONCLUSIONS

Microcapsules filled with EPA were successfully synthesized by *in situ* polymerization. Morphological analysis indicated that the microcapsule-formation process included emulsification, wall-formation, and wall-solidification stages. The healing efficiency of the solvents in terms of the healing time, amount, and degree of curing was related to the swelling process, as confirmed by manual healing experiments. The swelling curve was overlaid on the healing kinetics, and this indicated that crack healing was achieved as a result of solvent diffusion. The healing load reached a maximum value when the amount of healing agent was 0.5 μL, which was capable of filling the crack volume. Moreover, the healing performance under different curing conditions was related to the degree of swelling. The self-healing materials were realized by the addition of microcapsules filled with EPA into the matrix. The self-healing efficiency depended on the microcapsule concentration. The fracture toughness of the materials was fully restored to the original value when the microcapsule concentration was 10%. The fracture line in the healing interface was difficult to detect, and this suggested complete crack healing by the solvent.

Given that the solvent-promoted crack healing is based on a swelling mechanism, solvents with a higher diffusion rate and swelling capacity can heal cracks faster, and they have a higher healing efficiency for highly crosslinked matrixes. Improvements in the solvent healing system are necessary for practical application. In future research, we will focus on the selection of solvents with good swelling abilities for fast and efficient self-healing systems.

ACKNOWLEDGMENTS

The work was supported by the Natural Science Foundation of China (contract grant number 50775222). The authors thank Xiaodi Liu for helpful technical support.

REFERENCES

1. Gassan, J.; Dietz, T. *Compos. Sci. Technol.* **2001**, *61*, 157.
2. Li, M. C.; Ge, X.; Cho, U. R. *Macromol. Res.* **2013**, *21*, 519.
3. Li, M. C.; Zhang, Y. H.; Cho, U. R. *Mater. Des.* **2014**, *63*, 565.
4. Dry, C. *Smart Mater. Struct.* **1994**, *3*, 118.
5. White, S. R.; Sottos, N. R.; Geubelle, P. H.; Moore, J. S.; Kessler, M. R.; Sriram, S. R.; Brown, E. N.; Viswanathan, S. *Nature* **2001**, *409*, 794.
6. Toohey, K. S.; Sottos, N. R.; Lewis, J. A.; Moore, J. S.; White, S. R. *Nat. Mater.* **2007**, *6*, 581.
7. Burattini, S.; Colquhoun, H. M.; Greenland, B. W.; Hayes, W. *Faraday Discuss.* **2009**, *143*, 251.
8. White, S. R.; Moore, J. S.; Sottos, N. R.; Krull, B. P.; Cruz, W. A. S.; Gergely, R. C. R. *Science* **2014**, *344*, 620.
9. Brown, E. N.; Sottos, N. R.; White, S. R. *Exp. Mech.* **2002**, *42*, 372.
10. Brown, E. N.; White, S. R.; Sottos, N. R. *J. Mater. Sci.* **2004**, *39*, 1703.
11. Rule, J. D.; Sottos, N. R.; White, S. R. *Polymer* **2007**, *48*, 3520.
12. Kessler, M. R.; White, S. R. *J. Polym. Sci. Part A: Polym. Chem.* **2002**, *40*, 2373.
13. Rule, J. D.; Brown, E. N.; Sottos, N. R.; White, S. R.; Moore, J. S. *Adv. Mater.* **2005**, *17*, 205.
14. Jones, A. S.; Rule, J. D.; Moore, J. S.; White, S. R.; Sottos, N. R. *Chem. Mater.* **2006**, *18*, 1312.

15. Mauldin, T. C.; Rule, J. D.; Sottos, N. R.; White, S. R.; Moore, J. S. *J. R. Soc. Interface* **2007**, *4*, 389.
16. Liu, X.; Lee, J. K.; Yoon, S. H.; Kessler, M. R. *J. Appl. Polym. Sci.* **2006**, *101*, 1266.
17. Keller, M. W.; White, S. R.; Sottos, N. R. *Adv. Funct. Mater.* **2007**, *17*, 2399.
18. Keller, M.; White, S.; Sottos, N. *Polymer* **2008**, *49*, 3136.
19. Yin, T.; Rong, M.; Zhang, M.; Yang, G. *Compos. Sci. Technol.* **2007**, *67*, 201.
20. Yuan, Y. C.; Rong, M. Z.; Zhang, M. Q.; Chen, J.; Yang, G. C.; Li, X. M. *Macromolecules* **2008**, *41*, 5197.
21. Xiao, D. S.; Yuan, Y. C.; Rong, M. Z.; Zhang, M. Q. *Polymer* **2009**, *50*, 2967.
22. Yuan, Y. C.; Rong, M. Z.; Zhang, M. Q.; Yang, G. C. *Polymer* **2009**, *50*, 5771.
23. Yuan, Y. C.; Ye, X. J.; Rong, M. Z.; Zhang, M. Q.; Yang, G. C.; Zhao, J. Q. *ACS Appl. Mater. Interfaces* **2011**, *3*, 4487.
24. Ye, X. J.; Zhang, J. L.; Zhu, Y.; Rong, M. Z.; Zhang, M. Q.; Song, Y. X.; Zhang, H. X. *ACS Appl. Mater. Interfaces* **2014**, *6*, 3661.
25. Caruso, M. M.; Delafuente, D. A.; Ho, V.; Sottos, N. R.; Moore, J. S.; White, S. R. *Macromolecules* **2007**, *40*, 8830.
26. Caruso, M. M.; Blaiszik, B. J.; White, S. R.; Sottos, N. R.; Moore, J. S. *Adv. Funct. Mater.* **2008**, *18*, 1898.
27. Caruso, M. M.; Blaiszik, B. J.; Jin, H.; Schelkopf, S. R.; Stradley, D. S.; Sottos, N. R.; White, S. R.; Moore, J. S. *ACS Appl. Mater. Interfaces* **2010**, *2*, 1195.
28. Neuser, S.; Michaud, V.; White, S. R. *Polymer* **2012**, *53*, 370.
29. Blaiszik, B. J.; Baginska, M.; White, S. R.; Sottos, N. R. *Adv. Funct. Mater.* **2010**, *20*, 3547.
30. Jud, K.; Kausch, H. H.; Williams, J. G. *J. Mater. Sci.* **1981**, *16*, 204.
31. Kim, Y. H.; Wool, R. P. *Macromolecules* **1983**, *16*, 1115.
32. Wool, R. P. *Soft Matter* **2008**, *3*, 400.
33. Blaiszik, B. J.; Caruso, M. M.; McIlroy, D. A.; Moore, J. S.; White, S. R.; Sottos, N. R. *Polymer* **2009**, *50*, 990.
34. Manfredi, E.; Cohades, A.; Richard, I.; Michaud, V. *Smart Mater. Struct.* **2015**, *24*, 015.
35. Brown, E. N.; Kessler, M. R.; Sottos, N. R.; White, S. R. J. *Microencapsul.* **2003**, *20*, 719.
36. Fan, C.; Zhou, X. *Colloids Surf. A* **2010**, *363*, 49.
37. Yoshizawa, H.; Kamio, E.; Hirabayashi, N.; Jacobson, J.; Kitamura, Y. J. *Microencapsul.* **2004**, *21*, 241.
38. Neuser, S.; Michaud, V. *Exp. Mech.* **2014**, *54*, 293.
39. Santiago, D.; Fernández-Francos, X.; Ramis, X.; Salla, J. M.; Sangermano, M. *Thermochim. Acta* **2011**, *526*, 9.
40. Yue, C. Y. J. *Adhes.* **1986**, *20*, 99.